
Article:
Sweetman, A orcid.org/0000-0002-7716-9045, Harivyasi, SS orcid.org/0000-0002-2174-5226, Henry, J et al. (1 more author) (2020) Imaging and manipulation of adsorbed Pb adatom structures on the Si(100) surface by noncontact atomic force microscopy. Physical Review B, 102 (23). 235417. ISSN 2469-9950

https://doi.org/10.1103/physrevb.102.235417

Imaging and manipulation of adsorbed Pb adatom structures on the Si(100) surface by non-contact atomic force microscopy

Adam Sweetman,* Shashank S. Harivyasi, and Jack Henry
The School of Physics and Astronomy, The University of Leeds, Leeds, LS2 9JT, U.K.

Ioannis Lekkas
Diamond Light Source, Didcot Oxfordshire, OX11 0DE
(Dated: November 23, 2020)

We performed imaging and manipulation of epitaxially grown Pb adatom structures on the Si(100) surface by non-contact atomic force microscopy (NC-AFM) in ultra-high-vacuum (UHV) and at cryogenic temperatures. We observe several distinct contrast modes during imaging, which we assign to termination of the scanning probe tip by either a single Si, or single Pb, atom, via quantitative comparison of atomic resolution force spectroscopy experiments with ab initio density functional theory (DFT) simulations. We show that the Pb adatom structures can be controllably manipulated via mechano-chemical means, and identify a novel semi-deterministic manipulation strategy that arises from the combination of low temperature operation and the asymmetric diffusion barriers present on the Si(100) surface.

I. INTRODUCTION

On the nanometer scale, the forces across an inter-atomic, or inter-molecular junction, are determined by the chemical identity and precise bonding configuration of the atoms in the junction. Minor variations in the precise arrangement of these atoms can therefore produce dramatic changes in the resultant interaction, particularly if significant changes occur in the hybridisation of the atoms.

Non-contact atomic force microscopy (NC-AFM) remains one of the few experimental techniques capable of directly accessing inter-atomic forces on the single atom length scale [4] [5]. Recently, combining low temperature operation with controllably functionalised tips has resulted in an explosion of interest in its application to sub-molecular imaging [6] [7–9], which is typically performed by controllably reducing the chemical reactivity of the tip apex by absorption of a single carbon monoxide molecule. The same technique has recently shown that the difference in chemical reactivity of individual iron atoms may be mapped with high-resolution [10], highlighting how the coordination of a single atom modifies the resulting interatomic forces. Moreover, the ability of NC-AFM to directly access the atomic-scale tip-sample forces has provided critical insight into the mechanisms underpinning atomic manipulation experiments [4, 6, 11]

Imaging and manipulation of semiconductor systems using NC-AFM is motivated by two primary considerations. First, the ability to place single adatoms with atomic precision on a Si surface has a high degree of technical application, particularly with regard to the placement of dopant atoms [12–14]. Second, because of the strong chemical bonds usually formed between the semiconductor substrate and the adsorbate (atoms or molecules), it is possible to perform atomically precise manipulation experiments even at room temperature [15, 16]. In contrast, manipulation on metal substrates is usually limited to cryogenic temperatures, due to the relatively low diffusion barriers for similar absorbates on metal surfaces, a limitation which obviously narrows their technological applications.

Previous work has realised lateral and vertical interchange reactions, using the close approach of the scanning probe tip [15, 16]. More recently, similar techniques have been used to controllably lower the diffusion barrier between local potential minima for metal adatoms on the Si(111)-7x7 surface, allowing controlled assembly of metallic nanoclusters, atom by atom [17]. These protocols can also trigger an exchange reaction between a surface absorbed adatom and an intrinsic adatom of the surface [18]. These methods may, in principle, provide a route towards controlled atomic scale patterning of semiconductor surfaces, without a resist layer, even at room temperature.

Despite its greater technological relevance, the imaging of adsorbates on the Si(100) surface remains less explored by NC-AFM imaging. Notable exceptions are the identification of the structural and chemical identity of mixed adatom chains via combined NC-AFM and STM [3], imaging and manipulation of both Sn [19], and Mn adatom chains [20][21], and characterisation of intrinsic boron defects [22]. However, in none of these studies was the interaction of different types of scanning probe tip with the absorbed structures investigated in detail, nor was the range, and limitations, of the manipulation processes.

In this paper, we explore the imaging and manipulation of absorbed Pb adatom chains on the Si(100) surface as a prototypical system for exploring atomic scale interactions in semiconductor systems. We find the terminating atom of the scanning probe plays a key role in determining the nature of the tip - sample interaction, which in turn controls the observed contrast during imaging, and

* A.M.Sweetman@Leeds.ac.uk

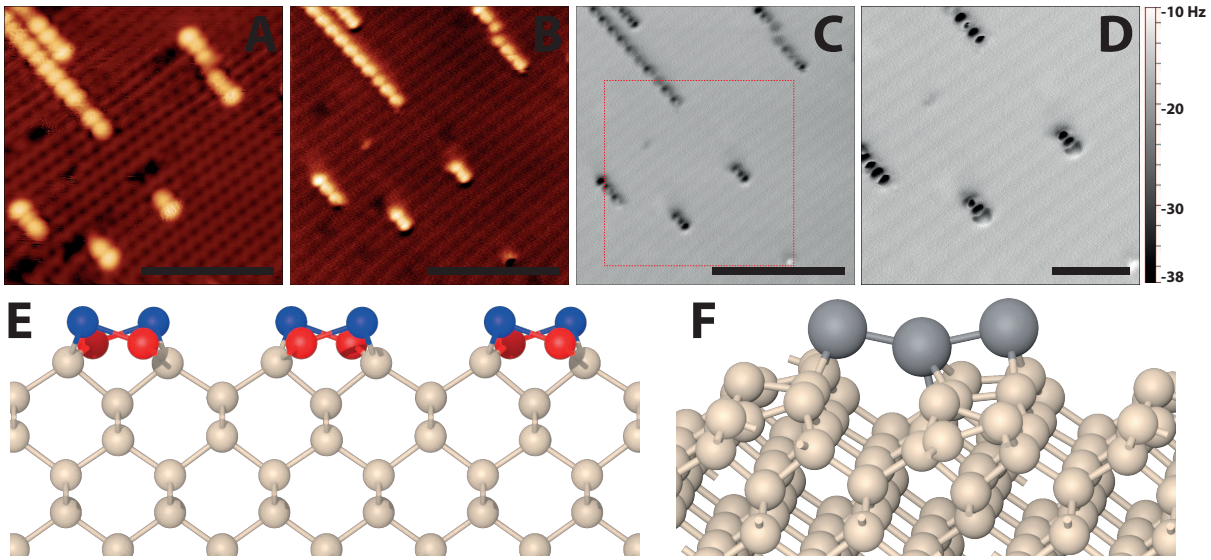

FIG. 1. A: Conventional STM image of the Si(100) surface with a low coverage of Pb chains V_{gap} = +1.6 V, B: Constant Δf NC-AFM image of the same chains Δf = -9 Hz, oscillation amplitude (A_0) = 0.1 nm, V_{gap} = 0 V. C: Simultaneously acquired pseudo constant height [1–3] Δf image. Scale bars 5 nm. D: High-resolution true constant height Δf image of the area highlighted in by the red square in C, Scale bar 2 nm E: Ball and stick model of the c(4x2) reconstruction of the Si(100) surface, the surface dimers are color coded - blue atoms are the 'up' atoms of the dimer, red atoms the 'down' atom of the dimer. F: Calculated ground state configuration of a small three Pb atom chain adsorbed on the Si(100).

manipulation modes. By comparison with state-of-the-art ab initio density functional theory (DFT) calculation, we tentatively assign the difference in imaging modes as arising from Si, and Pb terminated probes. Pb terminated probes demonstrate a surprisingly low reactivity, similar in magnitude to CO terminated tips, whereas Si probes exhibit a higher reactivity. By close approach of the tip we are able to demonstrate a range of different atomic scale manipulation strategies, some acting in a conventional, deterministic, mode, whereas others utilise a novel manipulation strategy, reliant on a combination of deterministic and constrained stochastic processes.

II. METHODS

A. Experimental methods

All experiments were performed in ultrahigh vacuum (UHV) (base pressure of 5x10^{-11} mbar or better) using a commercial Omicron Nanotechnology LT STM/NC-AFM in the qPlus configuration. Measurements were performed in a low temperature cryostat cooled to approximately 78 K using liquid nitrogen. Clean highly As doped n-type Si(100) samples were prepared by the standard method of flash heating via direct current to 1200°C, quickly cooling to 900°C and then slowly cooling to room temperature. A low coverage of Pb atoms was deposited via exposing the sample to a flux of Pb atoms from a high purity Pb sample (Goodfellows) mounted in a Mo crucible and heated by electron bombardment. During deposition the Si wafer was either at room temperature or cooled to ∼100 K. Deposition onto a cooled sample resulted in a higher proportion of metastable structures, and lateral manipulation experiments were more readily performed on samples prepared at low temeprature as compared to those prepared at room temperature. After deposition the sample was transferred directly into the scan head for imaging. We used a homebuilt qPlus sensor [23] with an etched tungsten tip attached to one tine of the tuning fork. These were introduced into the UHV chamber and then directly into the scan head without any preparation in UHV. The tips were prepared by standard STM methods, including tip pulsing and controlled crashes into the surface until good STM resolution is obtained. Only after achieving good STM contrast would we attempt NC-AFM imaging. Due to the preparation methods used, we assume the apex of our tip is terminated with either Si or Pb, rather than tungsten. All NC-AFM imaging was performed at 0 V_{gap} to avoid influence from the so-called "phantom force" [24] induced due to large tunnel currents, or any effect due to electronic crosstalk [25]. Constant height imaging was used to probe the complete range of interaction with a reduced risk of feedback instabilities. Due to the residual drift and creep at 78K a custom-built atom tracking unit [26, 27] was used in order to both measure, and then correct, thermal drift by applying feedforward correction in between each scan.

Quantitative force data was acquired by taking a Δf(z) measurement on a feature of interest (on curve), and also over the bare surface (off curve). The (off) data

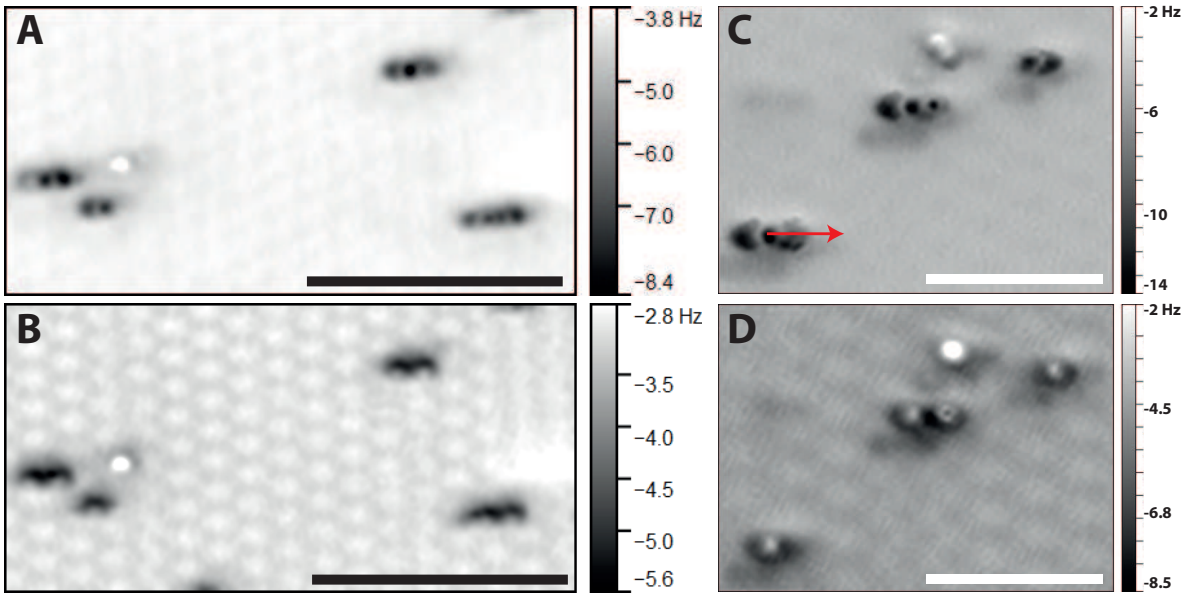

FIG. 2. A: Constant height Δf NC-AFM image taken with a tip showing 'Type I' contrast on a number of small Pb chains. B: Constant height Δf NC-AFM image of the same region taken with a tip showing 'Type II' contrast. Scale bars = 4 nm C: High resolution Constant height Δf NC-AFM image image of a different region taken with a tip showing 'Type I' contrast. After imaging the tip was approached -0.2 nm closer to the surface and moved over the path shown by the red arrow. D: After manipulation the crescent shaped feature has disappeared, and the tip now exhibits 'Type II' type contrast. Scale bar = 2 nm. A_0 = 0.2 nm, V_{gap} = 0 V in all images. A five-point Gaussian has been applied to all images to remove high frequency noise.

is then subtracted from the (on) data in order to produce a "short-range" Δf(z). This short-range Δf(z) was then inverted to force (F(z)) using the Sader-Jarvis algorithm [28]. Although we expect some small residual influence of the underlying substrate on our 'off' force curves (and hence expect them to systematically underestimate the true site specific forces), we prefer this 'on-versus-off' method (as used by Lantz et al.[29] and Ternes et al. [5]) to the much larger uncertainties that would be introduced by attempting to extract the site-specific forces via fitting of the long range background [30][31]. 3D Δf maps were acquired via the 'slice' method and de-convolved to site specific forces via the same method.

B. Computational methods

Force spectroscopy simulations were performed using density functional theory as implemented in the all - electron FHI - aims simulation package [32]. The Perdew–Burke–Ernzerhof functional [33] complemented with a van der Waals energy term (PBE+TS) was employed [34]. The calculations were performed using 'tight' settings on a 3 × 6 × 1 Γ-centered k-point grid. The criterion for converging self-consistent field cycles was 10^{-6} eV for the total energy and a given geometry was deemed to be relaxed when the maximum residual force component per atom computed to be less than 0.01 eV/Å for all unconstrained atoms.

For all simulations, we used a 12 atomic layer thick Si(100) slab with c(4×2) reconstruction on one side, and hydrogen termination on the other. In agreement with our previous work [11], our calculations found this reconstruction to be more stable than the p(2×2) reconstruction. After performing geometry relaxation on the slab once, all but top four Si atomic layers were constrained in subsequent relaxations. All relaxations were performed using 'light' settings followed by relaxation using 'tight' settings. Similarly, the three tips that we explored were allowed to fully relax in-vacuo and then their all but bottom 2 atomic layers were constrained in the subsequent relaxations.

The simulation cell containing tips had a surface area of 475Å^2 ensuring a minimum distance of 15Å between periodic images of Pb adatom(s) and of 7.6Å between Si atoms that constituted the (dimerized) tip. A vacuum of at least 11Å was placed above the tip to minimize spurious interaction between periodic images of the slab and the tip. To model a small adsorbed Pb chain, three adatoms of Pb were introduced in the cell gradually, allowing geometry relaxation of the slab to incorporate each new adatom; the second adatom formed an intradimer system [35] to which a third was added in order to create a monoadatom plus dimer system. This monoadatom plus intradimer configuration has been suggested by Jurczyszyn et al. [35] to be the stable configuration for Pb adatom chains with three or more atoms. Since longer chains would have required a substantial increase in the size of the simulation cell, we performed all simulations with tips on the Si surface with three Pb adatoms

in the unit cell.

Calculations to simulate tip approach were performed in a gradual manner, with resultant relaxed geometry from preceding step acting as the input geometry of the next – with the tip moved by the requiste vector in each step. Starting geometries were obtained by placing the tip at a height of 7Å ; where the height of tip is defined as the distance between the lowermost atom of the tip and the averaged height of the three Pb adatoms. This height was then reduced in a non-linear manner with step size reducing from 1Å (far from adatoms) to 0.2 Å (close to adatoms).

III. EXPERIMENTAL RESULTS

A. Comparison of STM and NC-AFM imaging

Conventional STM imaging of the sample after deposition of lead confirmed the growth of short chains of Pb dimers perpendicular to the direction of the buckled Si dimer rows - see Fig. 1 A. The structure and growth mode of metal chains on Si(100) has previously been well studied by scanning probe methods, and both STM [36–39] and NC-AFM [3, 19, 20] studies have shown that at low coverages many metal species self-assemble into chains which nucleate at a surface defect or step edge and grow perpendicular to the direction of the Si rows in dimer units. For Pb specifically, it is thought that chains terminated by a single Pb at the end of the chain are energetically favourable [35, 38]. Experiment and theoretical calculations also confirm that for Pb the dimers are buckled similar to the Si dimers of the surface reconstruction (Fig. 1 E-F), with charge transfer between the lower and upper atoms of the dimer [40, 41]. Previous NC-AFM studies have shown that the buckling structure of ad-dimers formed of Sn atoms can be manipulated [19], similar to native Si dimers [11] [42].

Constant Δf NC-AFM imaging of the same region shows broadly similar contrast (Fig. 1 B), with the Pb ad-dimers appearing topographically higher than the underlying substrate. However, simultaneously acquired pseudo constant height [1–3] imaging of the same region (Fig. 1 C) shows a more complex contrast. Here the difference in the buckling state of the up and down atoms of the Pb dimers are clearly visible. We note here that several of the Pb atoms terminating the chains display a distinct crescent shape. These features are more pronounced during constant height NC-AFM imaging at closer approach (Fig. 1 D). On the basis of data presented later in the paper, we assign these crescent features to single unpaired Pb atoms terminating the chains.

B. Contrast modes

Because contrast in NC-AFM arises explicitly via the chemical interaction between tip and probe, changing the nature of the tip termination can cause dramatic changes in the observed contrast.

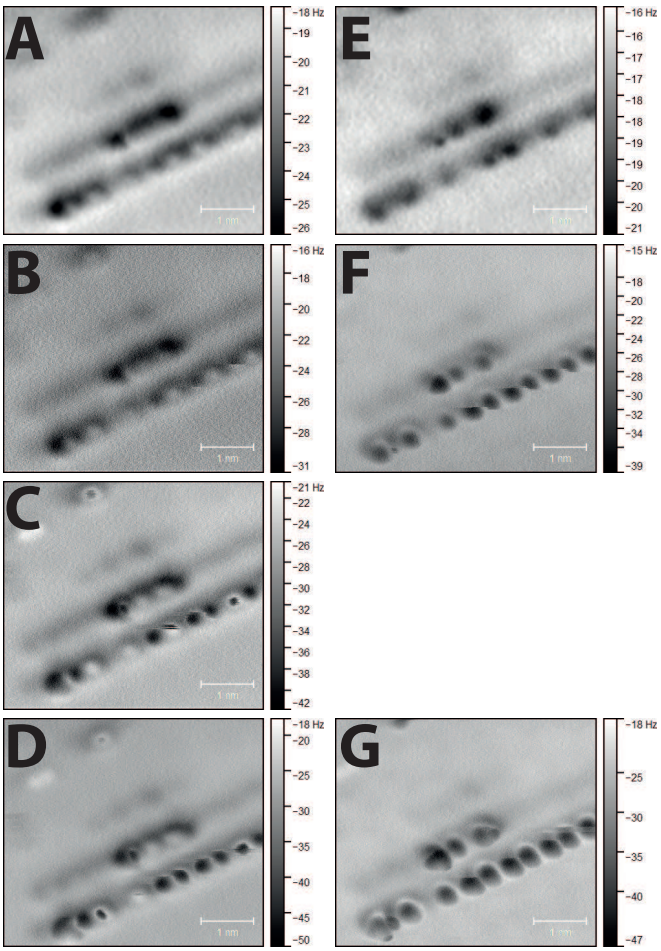

FIG. 3. (left column) A-D: Constant height Δf images taken at progressively closer tip-sample separation with Type Ia contrast. (right column) E-G Constant height Δf images taken at progressively closer tip-sample separation with a Type Ib contrast. A & E Imaging in the far field. Images B & F - closer approach ('slicing' indicates flipping of individual dimers by the scan). C: Image showing 'opening up' of bright atoms with the Type Ia tip. D & G at close approach a p(2x1) symmetric like phase appears due to constant flipping of the dimers. Images A and E have been filtered with a five-point Gaussian to remove high frequency noise. Note the faint 'shadow' above the chains is the result of a slight double tip. Scale bars = 1 nm in all images

Fig. 2 shows the two examples of the same region imaged with two different tips. In Fig. 2 A, a number of small chains are imaged with similar contrast to that observed in Fig. 1 D. After close approach with another chain outside the scan frame (not shown) the contrast changed to that shown in Fig. 2 B. Almost all of the stable imaging performed of these chains showed one of these characteristic imaging modes, and during close approach of the tip to the chains, it was on occasion possible to observe reversible switching between the two modes.

In order to help clarify the origin of the contrast we deliberately induced a contrast change via controlled approach of the tip, demonstrated in Fig. 2 C. Here two three atom chains, and a single dimer, are imaged in constant height mode. Subsequent to this image the tip was then positioned over the small chain in the lower left corner and moved -0.2 nm towards the surface (relative to the imaging height), and moved in the path indicated by the red arrow. During this motion an atomic manipulation event was indicated via a sharp jump in the Δf signal. Subsequent imaging of the same region after this close approach (Fig. 2 D) shows two key differences. First, the structure of the lower chain has changed compared to the centre chain, indicating the pickup of one of the constituent atoms. Second, the image contrast over the entire scan has dramatically changed. The crescent shaped features in Fig. 2 C have been observed to move spontaneously between closely spaced chains (see Supporting information [43]), and prior structural models of short chains [35] suggest some chains should be terminated with single adatoms. On this basis, if we assign the crescent features as corresponding to single Pb adatoms we suggest that the change in contrast arises from a pickup of a single Pb atom onto the tip.

The imaging modes we observe fall into two broad categories. Fig. 2 A and C show contrast we term Type Ia and Type Ib, whereas Fig. 2 B and D show a contrast we term Type II. The justification for the subdivision of Type I contrasts arises from the observation of small tip changes resulting in a switch between the two modes, and the fact that depending on the tip-sample separation, and resolution, the modes can be quite difficult to distinguish without careful height dependent imaging. This is highlighted in Fig. 3, which shows the same area imaged at different tip separations with both Type Ia and Type Ib tips. The key difference, which we return to later, is that at relatively large tip-sample separations Type Ia tips show a repulsive interaction over one of the dimer atoms before becoming attractive, whereas Type Ib demonstrates an increasingly attractive interaction over the centre of the atoms.

The distinction between Type I and Type II is more straight forward. Type I (Fig. 2 C) tips have crescent shaped end atoms, and atoms within the chain image primarily as dark (attractive) lobes in constant height imaging (although as we note, the evolution of the contrast in Type I with varying tip-sample height can be complex - see also Supporting information [43]). In Type II (Fig. 2 D), we do not observe crescent shaped atoms, instead the up and down atoms of the dimers image as bright and dark spots (we discuss the assignment of the up and down atoms in the next section).

C. Quantitative force spectroscopy

In order to identify the origin of the different contrast modes, we performed site-specific force spectroscopy with

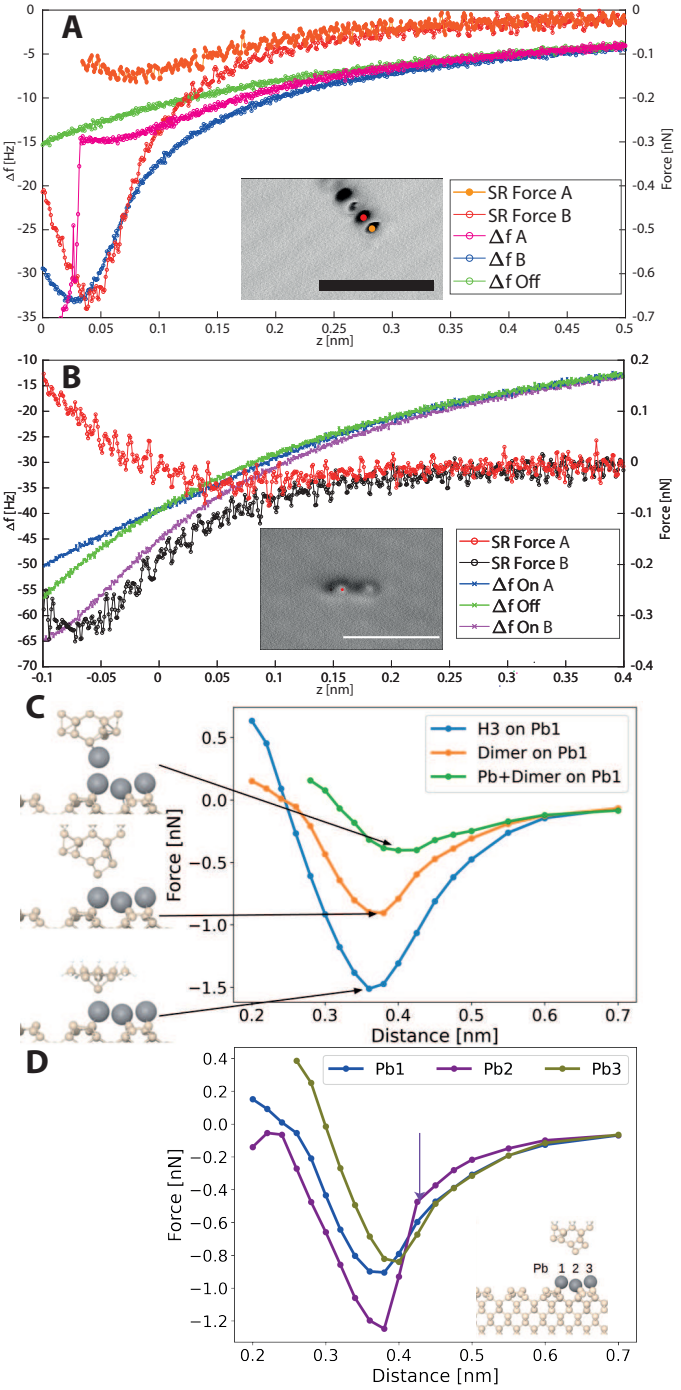

FIG. 4. A: $\Delta f(z)$ and F(z) curves acquired over both atoms of a Pb dimer with a tip showing 'Type Ia' contrast. Inset - Constant height Δf NC-AFM with positions of F(z) curves marked. Scale bar 2 nm. B: As for A, but with a tip showing 'Type II' contrast. Inset - Constant height Δf image with positions of F(z) curves marked. Scale bar 1 nm. C: F(z) approach curves calculated via DFT for three different Si and Si/Pb tip clusters (shown on the left) over the up Pb atom of a Pb dimer. D: F(z) DFT approach curves over all three atoms of the Pb chain, performed with a dimer Si tip cluster.

both types of tips over various locations on each chain, the results of which are shown in Fig. 4 A and B. First, it is important to discuss the two sites of interest within the Pb chain. The assembly of the Pb chains on the Si surface results in a buckling of the Pb dimers, similar to that on the Si surface itself. As a result, there is an "up", and "down" atom, which have different physical, and chemical environments, primarily as a result of the charge transfer between the atoms in the dimer. On the Si surface this charge transfer has previously been estimated to be on the order $0.3e$ transferred from the lower atom to the upper atom [40, 41]. In our calculations we find a similar transfer of approximately 0.1 to 0.15e (depending on the charge counting method) from the lower to upper atoms on both the Si, and Pb, dimers.

This geometric, and electronic, difference results in a significant difference in the tip-sample forces observed over each atom, both quantitatively and qualitatively. Turning first to spectra with a Type Ia tip (Fig. 4 A); spectra taken on the "dark atom" of the dimer (red curve) demonstrate a relatively strong force interaction, on the order of 600 to 700 pN, this is in line with the magnitude of forces previously observed during similar experiments on Sn adatoms [19]. Conversely, force spectroscopy performed on the "bright" atom with a dark centre (orange curve) show much smaller turnarounds in the force (approximately 150 pN). However, after the force turning point we see a very large jump in the measured frequency shift value. The frequency shift after this point has not been converted to force due to known issues with the inversion algorithm in the presence of such discontinuities [44, 45], but based on the magnitude of the frequency shift alone, it seems plausible that the force in this region would be of a similar magnitude to that over the "dark atom" of the dimer. Definitive assignment of the up and down atom in this case is challenging and we return to discussion of this later.

Spectroscopy performed using a tip demonstrating Type II imaging is somewhat easier to interpret (Fig 4 B). Force spectroscopy over the "dark" atom of the dimer (black curve) shows a moderate force turnaround, of approximately 350 pN. Force spectroscopy on the "bright" atom of the dimer (red curve) shows a very small force turnaround (less than 50 pN). Further approach over the "bright" atom can also result in a jump in the frequency shift, which may be understood as a "push" type manipulation resulting in reversible switching of the dimer (see Fig. 7 and Section IV C). The spectra of Type II tips on the chains can be understood to a first approximation relatively easily if we assume a "passivated" type tip interaction similar to a CO terminated tip [6**?**] (see supporting information [43]).

For Type Ib tips, only a limited amount of spectroscopy data is available (discussed in Fig. 8). From this data we are unable to determine the peak interaction force, but can state that it exceeds 0.4 nN. We can also confirm the qualitative observation from imaging that no repulsive interaction is observed (Fig. 3).

Although there is a clear quantitative difference in the magnitude of the peak force over each site between the Type Ia and Type II tip types, there are further qualitative differences in their behaviour which we outline here.

If we assume that for both tips the dark atoms represent the down atoms of the dimer than we can relatively easily understand the full spectra over this position for both tips - i.e. there is an attractive part of the interaction due to chemical bonding and dispersion interactions, and at close approach this becomes repulsive as Pauli repulsion becomes dominant, differing only quantitatively from the well studied silicon-silicon interaction [29]. Therefore, the complexity in interpretation arises from understanding the interaction over bright atoms, which we will assume corresponds to the up atom of the dimer.

We first consider the Type II contrast. When the tip approaches close over the up atom we see a repulsive interaction and then a jump in Δf (see Fig. 7 E), which we can interpret as resulting in a change in the configuration of the Pb dimer under the tip via a push type interaction, on the basis of subsequent scans of the same region which show a change in the dimer configuration.

At first glance it may appear that Type Ia interactions can be understood in the same way, but closer inspection of scans at close approach suggests a more complex interpretation is necessary. Instead of repeated 'flip' events, we instead observe a phenomena similar to that described during imaging of adatoms on the Si(111)-7x7 surface with passivated (but undefined) tips [31] (see also Supporting information [43]). That is, we observe a repulsive interaction followed by an 'opening up' of a dark attractive feature in the centre of the atom. This results in a dark (attractive) feature surrounded by a bright (repulsive) halo. Although we can observe dimers being perturbed during imaging with Type Ia tips (Fig. 3 B), approach into the strongly interacting regime not seem to result in a simple, clearly defined, reversible switching of the whole dimer unit as for the interaction described for the Type II tips.

D. Simulated spectroscopy

Because of the complex nature of the different contrast modes, and the fact that our tips prepared by controlled collisions with the surface, we simulated force spectroscopy with a variety of small Pb, and Si, terminated clusters in order to elucidate the likely classes of tip that could result in the behaviour described in the previous section.

First, we examined the force-distance evolution over the 'up' atom of the Pb dimer of a three atom chain with three prototypical tip clusters, a highly reactive 'H3' Si-terminated tip , a 'dimerised' Si-terminated tip, and a Pb-terminated dimerised tip. The results of these simulations are shown in Fig. 4 C. Each tip produced qualitatively similar behaviour, with an attractive interaction

far from the Pb atom, which then turns around and becomes repulsive at close approach. There are however strong quantitative differences between the three tips. As expected the H3 tip reacts strongly with the Pb atom, forming a chemical bond with a peak force around -1.5 nN. The dimerised Si tip reacts less strongly, with a peak force around -0.8 nN, and the Pb terminated tip interacts very weakly, with a peak force of around -0.3 nN.

These results provide supporting evidence to the hypothesis that Type II contrast arises from Pb terminated tips, since we observe the likely pickup of a Pb adatom resulting in a switch from Type I to Type II contrast, and force spectroscopy with tips showing Type II contrast results in quantitatively similar forces to the results of simulated spectroscopy with a Pb terminated tip. These results also suggest that none of our experimentally observed tips are of the highly reactive H3 type. The intermediate tip-sample forces suggest that Type I and Ib tips are more likely to be of the dimerised Si class.

On this basis, we explored the behaviour of the dimerised Si tip over the other atoms in the chain (Fig. 4 D). The three atoms of the chain have different chemical environments. Atom 1 is the 'up' atom of a Pb dimer, atom 2 is the 'down' atom of a Pb dimer and atom 3 is an 'unpaired' adatom. The force curve over atom 3 is very similar to that over atom 1 (described in detail above), and so we do not discuss it further here. The interaction over atom 2 is qualitatively different - at the position of the arrow a sharp increase in force occurs, and examination of the geometries during the spectroscopy shows that this is the result of the Pb dimer 'flipping' - i.e. the lower atom jumps up into contact with the tip.

This behaviour is qualitatively the same as that observed with Type Ib tips, reproducing the well understood 'dimer flip' mechanism explored previously [19, 42]. However, it is important to highlight that this behaviour is qualitatively different from that observed experimentally for Type Ia tips. In the experimental spectra for Type Ia tips (Fig. 4 A), the jump in force occurs *after* the force turnaround - i.e. in the repulsive force regime. This force profile was also observed on Si(111)-7x7 with an unspecified 'passivated' tip [31]. However, we emphasise that we can rule out a simple passivated (e.g. CO terminated) tip, as such a tip would not produce the large attractive force recorded over the lower atom of the dimer. Consequently, while we can conclude on the basis of the magnitude of the forces on the lower atom that the Type Ia is reactive at close tip-sample distances, there is some aspect of the interaction that is not captured in our simulation. The most plausible explanation is that due to the limited number of tip clusters we have been able to examine, there exists another hybrid Si/Pb tip structure which could reproduce the observed force profile, but we also cannot rule out a limitation in the capabilities of DFT to accurately model this particular interaction with our chosen set of functionals.

E. Summary of tip assignments

Before considering manipulation, it is helpful to summarise the classification of the imaging and tip assignments. Briefly, we assign our observations into three tip classifications; Type Ia, Type Ib, and Type II. Type Ia and Ib display broadly similar imaging at some tip-sample heights but have subtly different behaviours at close approach. Type II tips demonstrate a qualitatively different contrast and are easily identified. Switches between Type I and Type II imaging can be induced by close approach to the Pb chains, suggesting the different contrasts arise from a change in the terminating atom from Si to Pb. Our simulated spectroscopy shows good agreement for Pb terminated tips compared to experimental results obtained with Type II tips. For Si terminated tips there is good agreement in the overall magnitude of the forces compared to experimental results with Type Ib tips, but they do not reproduce the complex behaviour observed experimentally in the repulsive regime over some of the atoms in the Pb dimers for Type Ia tips.

IV. MANIPULATION

During close approach of the tip to the Pb chains, atomic manipulation events of different types were observed. Below these are described and categorised into several classes. In the first, conventional lateral manipulation, the lateral positions of certain dimer units can be modified with atomic precision by moving the tip in a horizontal direction at close approach. In the second, a novel lateral manipulation scheme is shown, in which the lateral positions of single atoms are modified deterministically and then released in an asymmetric potential that takes advantage of the residual thermal energy available at 78 K to transport atoms over a large distance and spontaneously form new structures. Lastly, we show that manipulation of the "state" of the chain (i.e "dimer flipping") may be induced by vertical approach of the tip such that the configuration of the chain changes, but without displacing the atoms laterally.

A. Deterministic Lateral Manipulation

Lateral manipulation via the "dragging" of atoms across the surface with an STM tip is a routine manipulation strategy for absorbed metal adatoms on metal surfaces [46], and NC-AFM investigation of these systems via similar protocols have elegantly demonstrated the ability to measure the force needed to move an atom [4].

Of particular relevance is the recently demonstrated manipulation of epitaxially deposited Pb, Sn, Ag, and Au atoms at room temperature, which utilises the trapping of atoms in surface defined local potentials to allow

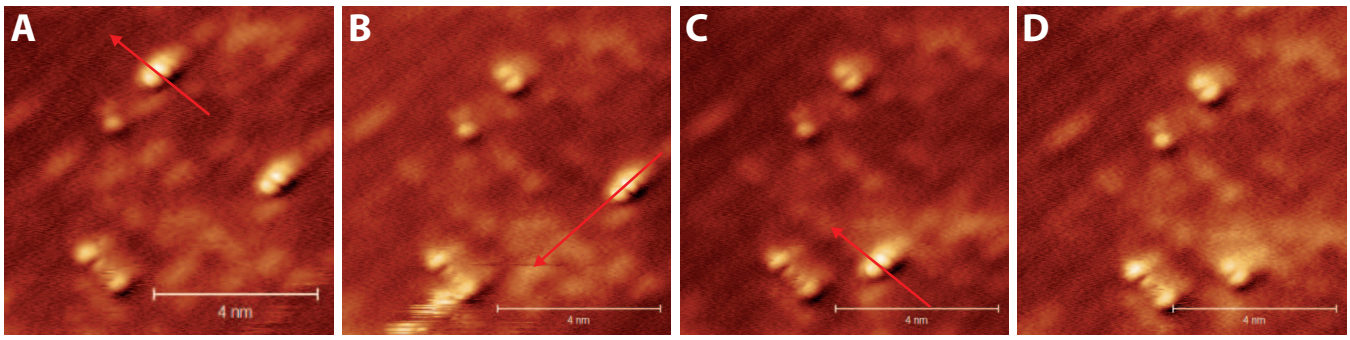

FIG. 5. A: Constant Δf NC-AFM image sequence showing manipulation of metastable Pb dimers. Manipulation performed in constant height at a ΔZ of -0.1 nm relative to imaging setpoint. Manipulation path shown by red arrow. B: As a result of the manipulation the dimer has rotated. Additional manipulation then performed on second dimer. C: Second dimer has been displaced laterally along the row. D: Second dimer has been rotated by additional manipulation. Δf = - 21 Hz, A_0 = 0.1 nm, V_{gap} = 0 V. Scale bar = 4 nm in all images.

assembly of atomically defined clusters even when the atoms are locally mobile on the surface [47] [17].

The results presented in this paper, acquired at intermediate temperatures (78K) provide an interesting prototypical system with which to investigate the barriers for movement and diffusion of small adatom clusters. In Fig. 5, the results of several lateral manipulations on two Pb dimers are shown, via close approach of the tip during lateral movement. These data show that the position of a single dimer can be modified up and down a single dimer row (via tip motion parallel to the Si dimer row direction), and its rotational orientation can also be switched (via movement of the tip perpendicular to the Si row direction). It has previously been shown that the diffusion barrier along the rows is significantly lower than across the rows for small adatom clusters [39] [48, 49], a point we return to in the next section.

We note that the Pb dimers here are adsorbed in a metastable configuration on top of the Si dimers, which may make them more amendable to manipulation. We were occasionally able to induce motion of a single dimer across the rows during very close approach of the tip, but this often induced changes to the tip state and was not highly reproducible, which is in line with the expected higher barrier for motion between rows

B. Novel Manipulation

Although the Pb dimers are positionally stable at 78 K, the same is not true of unpaired Pb adatoms. Unpaired adatoms are occasionally imaged diffusing along the rows for samples prepared at low temperature (see Supporting information [43]), and it is thought that these are adatoms that are trapped locally within a single row by defects and step edges, and hence unable to pair with as an existing chain or another adatom. As a result we only observe these diffusing species natively at relatively low chain coverages. However, even adatoms that have

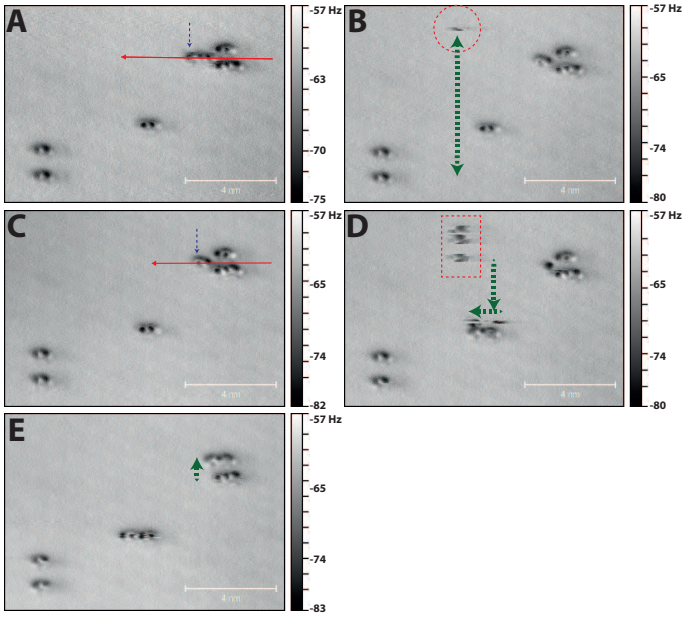

FIG. 6. A: Constant height Δf NC-AFM image of four dimers and two short chains of three atoms. The atom indicated by the blue arrow was targeted for manipulation. The tip was approached -0.12 nm closer to the surface, and moved over the path indicated by the red arrow. B: As a result of the manipulation the targeted atom has disappeared, and can be seen diffusing in the row where the manipulation was terminated (highlighted by red circle). The subsequent diffusion path indicated by the dashed green arrow. C: An additional atom is targeted for manipulation - same key as A. D: The second manipulated atom diffuses down the row and along the pre-existing chain, forming a metastable structure with the first diffusing atom (first atom highlighted by red rectangle). E: Note that spontaneous movement of the adatoms results in both a stable two dimer chain (centre) and two chains of three atoms (top right) which have formed as the result of the motion of the lone unpaired Pb adatom which remained the top right cluster. No further changes were observed during subsequent imaging. A_0 = 0.1 nm, V_{gap} = 0 V. Scale bar = 4 nm in all images.

adsorbed at a dimer chain can occasionally be observed to jump position between two closely spaced chains over long time periods (see supporting information [43]).

The stability of single dimers and longer chains, combined with the thermal mobility of unpaired adatoms (but with their diffusion strongly confined along the direction of the dimer rows), provides an unusual combination of energetic barriers. As shown in Fig. 6 this allows a combination of deterministic (i.e. directed directly by the tip motion), and "stochastic", (i.e. guided by thermal motion of the atom) manipulation strategies.

In the sequence shown, single adatoms are pulled out of a small cluster of chains, and deposited in a new dimer row. When only a single atom is deposited into the row, it subsequently diffuses freely, but the addition of a second atom into the same row allows the two adatoms to coalesce and form a stable structure adjacent to an existing dimer in the centre of the image. We highlight that because in the images shown in Fig. 6 the scan direction is always bottom to top, the transport of atoms from the top right to centre of the image cannot occur due to "dragging" of the atoms via the tip, as the tip motion is never in this direction. Furthermore the brief appearance and disappearance of the features in the target row in Fig. 6 B and D, is indicative of a diffusing atom briefly appearing under the tip during thermally induced motion, and hence we have a high degree of confidence that the transport does indeed result from the residual thermal energy at 78 K. These observations open up the possibility for combined manipulation strategies, where mass transport can be achieved more rapidly, but still with atomic precision, by depositing atoms into a confined energetic potential and then allowing thermal motion to transport them to defined binding sites where a predetermined reaction occurs.

The observation that we see adatom, but not ad-dimer, motion at 78K suggests that the diffusion barriers for the two must be qualitatively different. Although this makes sense intuitively we note that previous DFT based estimates of the energy barriers for Pb adatom and ad-dimer diffusion are very similar at 0.31eV and 0.32eV respectively [48, 50]. On the basis of our results it appears that the barrier for adatom diffusion may require re-evaluation, but we note that at 78K small uncertainties in barrier calculations can result in many orders of magnitude difference in expected lifetime (e.g. a simple Arrhenius estimate of the residency lifetime based on the calculated barriers suggests a 50meV uncertainty in barrier height will result in a three orders of magnitude difference in expected lifetime), and so it is possible even high quality simulation may not provide the accuracy needed for even a qualitative prediction of the expected behaviour.

We suggest there may be the potential for combining this modality with "gating" type manipulation strategies as described previously for metal adatoms on the Si(111)-7x7 surface [47], as it may be possible that the thermal motion of atoms between rows could be triggered by positioning the tip at specific locations in analogy to the "gating" of adjacent unit cells on Si(111).

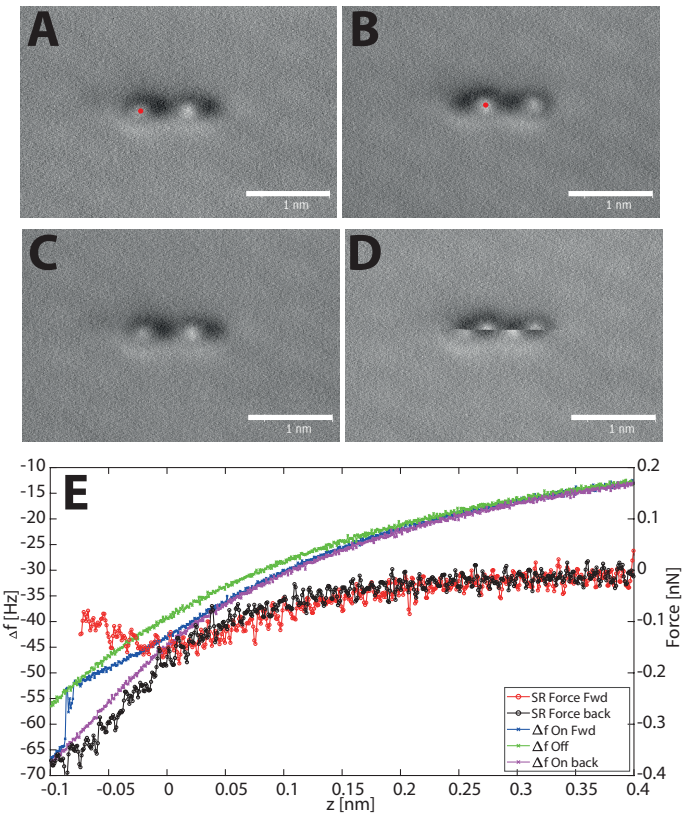

FIG. 7. A: Constant height Δf image (taken using a a tip showing Type II contrast) of a two dimer chain of Pb adatoms. Δf (z) spectroscopy was performed over the bright atom of the left hand dimer (position indicated by red dot), resulting in a change in the configuration of both dimers (i.e. coupled flipping - see panel B). B: Similar spectroscopy on the new bright atom of the dimer reverses the manipulation - see panel C. D: Example of spontaneous (scan induced) manipulation, again both dimers are observed to flip together. E: Representative $\Delta f(z)$ and resultant F(z) spectroscopy obtained during a dimer flip. The force after the jump in Δf is not plotted due to invalidity of the inversion algorithm in this regime. Nonetheless it is clear the manipulation occurs in the repulsive branch of the force curve - i.e. it is the result of a 'push' type manipulation. Scale bar = 1 nm in all images.

C. Dimer state manipulation

As noted in Section III C, during force spectroscopy of the chains, we occasionally observed sharp transitions in the frequency shift signal at close approach. By carefully controlling the imaging height, and the tip sample separation during the force spectroscopy, it was possible to induce reversible changes in the configuration of the dimer chains. Examples of this are shown in Fig. 7 and Fig. 8. Turning first to Fig. 7, performed using a tip showing Type II contrast. With a tip of this type, manip-

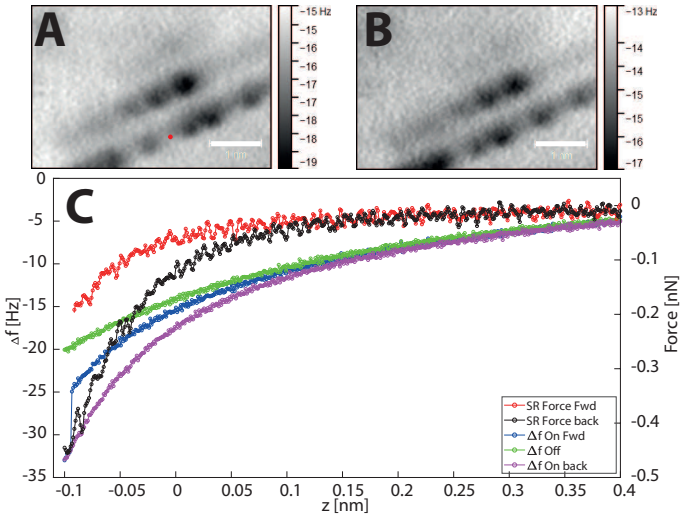

FIG. 8. A: Constant height Δf image (taken using a a tip showing Type Ib contrast) of short dimer chain of Pb adatoms (taken at large tip-sample distance to prevent perturbation of the dimer chain during scanning). A five-point Gaussian smooth has been applied to reduce high frequency noise. Δf (z) spectroscopy was performed over the down atom a dimer (position indicated by red dot), resulting in a change in the configuration of only the selected dimer. B: Same area after manipulation showing modified chain configuration. C: $\Delta f(z)$ and resultant F(z) spectroscopy obtained during the dimer flip. The force after the jump in Δf is not plotted due to invalidity of the inversion algorithm in this regime. Nonetheless it is clear the manipulation occurs in the attractive branch of the force curve - i.e. it is the result of a 'pull' type manipulation. Scale bar = 1 nm in both images.

ulation could only be induced by "push" type interaction which occurred after the turnaround in the F(z) curve, suggesting a transition was induced due to the repulsive forces between tip and sample. This is in contrast to the "pull" type manipulation identified for Si tips on Si and Sn dimers [11, 42] [19], where manipulation was induced by approaching the lower atom of the dimer. This suggests that when the tip-sample chemical interaction is inhibited, "push" type manipulations of this type are more likely to be responsible for introducing conformational changes in semiconductor systems. In contrast, in Fig. 8, performed with a Type Ib tip, the manipulation occurs in the attractive regime, suggesting a conventional, 'pull' type manipulation.

Inspecting the results of the manipulations, there are other qualitative difference. In Fig. 7 the confirmation of the second dimer in the chain is also modified, whereas in Fig. 8 only the targeted dimer has flipped. It is not trivial to determine whether this difference in behaviour is due to the different nature of the manipulation protocol/type, or differences in the local environment of the chain, as it is known that the stability of the dimers is modified by the length of the overall chain in which they exist. It is also possible that the elevated temperature may allow small energy barriers to be crossed, in contrast to previous work performed primarily at 5K [19, 42]. Only a further investigation, in a range of different local environments will permit this to be elucidated conclusively, and even more elaborate behaviours may be possible if mixed element hetro-chains are grown.

V. CONCLUSIONS

We have presented imaging and manipulation of Pb adatoms and ad-dimers on the Si(100) surface at 78 K using NC-AFM. Different contrast modes arise as the result of different tip terminations. The chemical identity of the terminating apex of the tip results in quantitative and qualitative differences in imaging, and a complex evolution in the tip-sample force for some tips points to a non-trivial interaction mechanism at close approach. Metastable ad-dimers can be manipulated with atomic precision via direct mechano-chemical interaction with the tip. Using the combination of asymmetric diffusion potential and intermediate substrate temperature it is possible to trap and release atoms to perform a semi-deterministic self assembly of new nanostructures. These results provide another mechanism by which single atoms may be manipulated on semiconductor surfaces, and may have application in the placement of single dopants with atomic precision via SPM techniques. However, a complete understanding of the tip-sample forces remains as an area for future work.

VI. ACKNOWLEDGEMENTS

We acknowledge support for computing time from EPSRC via the Tier 2 HPC facility HPC Midlands+. Adam Sweetman acknowledges support via a Royal Society University Research Fellowship, the ERC Grant 3DMOSHBOND, and from the Leverhulme Trust via fellowship ECF-2013-525. We thank Philip Moriarty, University of Nottingham, for valuable comments on the manuscript.

[1] C. Chiutu, A. M. Sweetman, A. J. Lakin, A. Stannard, E. Al, S. Jarvis, L. Kantorovich, J. L. Dunn, and P. Moriarty, Precise Orientation of a Single C_ {60} Molecule on the Tip of a Scanning Probe Microscope, Phys. Rev. Lett. **108**, 268302 (2012).

[2] C. Moreno, O. Stetsovych, T. K. Shimizu, and O. Custance, Imaging Three-Dimensional Surface Objects with Submolecular Resolution by Atomic Force Microscopy,

Nano Lett. **15**, 2257 (2015).
[3] M. Setvín, P. Mutombo, M. Ondráček, Z. Majzik, M. Švec, V. Cháb, I. Ošt'Ádal, P. Sobotík, and P. Jelínek, Chemical identification of single atoms in heterogeneous III-IV chains on Si(100) surface by means of nc-AFM and DFT calculations, ACS Nano **6**, 6969 (2012).
[4] M. Ternes, C. P. Lutz, C. F. Hirjibehedin, F. J. Giessibl, and A. J. Heinrich, The force needed to move an atom on a surface., Science **319**, 1066 (2008).
[5] M. Ternes, C. González, C. P. Lutz, P. Hapala, F. J. Giessibl, P. Jelínek, and A. J. Heinrich, Interplay of Conductance, Force, and Structural Change in Metallic Point Contacts, Phys. Rev. Lett. **106**, 16802 (2011).
[6] L. Gross, F. Mohn, N. Moll, P. Liljeroth, and G. Meyer, The Chemical Structure of a Molecule Resolved by Atomic Force Microscopy, Science (80-.). **325**, 1110 (2009).
[7] A. Sweetman, N. R. Champness, and A. Saywell, On-surface chemical reactions characterised by ultra-high resolution scanning probe microscopy, Chem. Soc. Rev. 10.1039/d0cs00166j (2020).
[8] L. Gross, B. Schuler, N. Pavliček, S. Fatayer, Z. Majzik, N. Moll, D. Peña, and G. Meyer, Atomic Force Microscopy for Molecular Structure Elucidation, Angew. Chemie - Int. Ed. **57**, 3888 (2018).
[9] S. P. Jarvis, Resolving intra- and inter-molecular structure with non-contact atomic force microscopy, Int. J. Mol. Sci. **16**, 19936 (2015).
[10] J. Berwanger, S. Polesya, S. Mankovsky, H. Ebert, and F. J. Giessibl, Atomically Resolved Chemical Reactivity of Small Fe Clusters, Phys. Rev. Lett. **124**, 096001 (2020).
[11] A. Sweetman, S. Jarvis, R. Danza, J. Bamidele, E. Al, S. Gangopadhyay, G. A. Shaw, L. Kantorovich, and P. Moriarty, Toggling Bistable Atoms via Mechanical Switching of Bond Angle, Phys. Rev. Lett. **106**, 136101 (2011).
[12] S. R. Schofield, N. J. Curson, M. Y. Simmons, F. J. Rueß, and E. Al, Atomically precise placement of single dopants in Si, Phys. Rev. Lett. **91**, 136104 (2002).
[13] M. Fuechsle, J. A. Miwa, S. Mahapatra, H. Ryu, S. Lee, O. Warschkow, L. C. L. Hollenberg, G. Klimeck, and M. Y. Simmons, A single-atom transistor., Nat. Nanotechnol. **7**, 242 (2012).
[14] B. Weber, S. Mahapatra, H. Ryu, S. Lee, a. Fuhrer, T. C. G. Reusch, D. L. Thompson, W. C. T. Lee, G. Klimeck, L. C. L. Hollenberg, and M. Y. Simmons, Ohm's Law Survives to the Atomic Scale, Science (80-.). **335**, 64 (2012).
[15] Y. Sugimoto, M. Abe, S. Hirayama, N. Oyabu, Ó. Custance, S. Morita, and O. Custance, Atom inlays performed at room temperature using atomic force microscopy, Nat. Mater. **4**, 156 (2005).
[16] Y. Sugimoto, P. Pou, O. Custance, P. Jelinek, M. Abe, R. Perez, and S. Morita, Complex Patterning by Vertical Interchange Atom Manipulation Using Atomic Force Microscopy, Science (80-.). **322**, 413 (2008).
[17] E. Inami, I. Hamada, K. Ueda, M. Abe, S. Morita, and Y. Sugimoto, Room-temperature-concerted switch made of a binary atom cluster, Nat. Commun. **6**, 6231 (2015).
[18] A. Yurtsever, M. Abe, S. Morita, and Y. Sugimoto, Atom manipulation method to substitute individual adsorbate atoms into a Si(111)-(7 7) substrate at room temperature, Appl. Phys. Lett. **111**, 10.1063/1.5008503 (2017).
[19] A. Sweetman, I. Lekkas, and P. Moriarty, Mechanochemical manipulation of Sn chains on Si(100) by NC-AFM, J. Phys. Condens. Matter **29**, 10.1088/1361-648X/29/7/074003 (2017).
[20] R. Villarreal, C. J. Kirkham, A. Scarfato, D. R. Bowler, and C. Renner, Towards surface diffusion potential mapping on atomic length scale, J. Appl. Phys. **125**, 10.1063/1.5091736 (2019).
[21] R. Villarreal, M. Longobardi, S. A. Koster, C. J. Kirkham, D. Bowler, and C. Renner, Structure of Self-Assembled Mn Atom Chains on Si(001), Phys. Rev. Lett. **115**, 256104 (2015).
[22] A. Sweetman, S. Gangopadhyay, R. Danza, N. Berdunov, and P. Moriarty, qPlus atomic force microscopy of the Si(100) surface: Buckled, split-off, and added dimers, Appl. Phys. Lett. **95**, 063112 (2009).
[23] I. Lekkas, PhD Thesis: An analysis of atomic manipulation , intermolecular resolution and the artefacts of dynamic force microscopy, (2017).
[24] A. Weymouth, T. Wutscher, J. Welker, T. Hofmann, and F. Giessibl, Phantom Force Induced by Tunneling Current, Phys. Rev. Lett. **106**, 226801 (2011).
[25] Z. Majzik, M. Setvín, A. Bettac, A. Feltz, V. Cháb, and P. Jelínek, Simultaneous current, force and dissipation measurements on the Si(111) 7x7 surface with an optimized qPlus AFM/STM technique, Beilstein J. Nanotechnol. **3**, 249 (2012).
[26] P. Rahe, J. Schutte, W. Schniederberend, M. Reichling, M. Abe, Y. Sugimoto, and A. Kuhnle, Flexible drift-compensation system for precise 3D force mapping in severe drift environments, Rev. Sci. Instrum. **82**, 063704 (2011).
[27] M. Abe, Y. Sugimoto, O. Custance, S. Morita, and et Al, Room-temperature reproducible spatial force spectroscopy using atom-tracking technique, Appl. Phys. Lett. **87**, 173503 (2005).
[28] J. E. Sader and S. P. Jarvis, Accurate formulas for interaction force and energy in frequency modulation force spectroscopy, Appl. Phys. Lett. **84**, 1801 (2004).
[29] M. A. Lantz, H. J. Hug, R. Hoffmann, P. J. A. van Schendel, P. Kappenberger, S. Martin, A. Baratoff, H.-J. Guntherodt, and H. J. Güntherodt, Quantitative Measurement of Short-Range Chemical Bonding Forces, Science (80-.). **291**, 2580 (2001).
[30] S. Kuhn and P. Rahe, Discriminating short-range from van der Waals forces using total force data in noncontact atomic force microscopy, Phys. Rev. B **89**, 235417 (2014).
[31] A. Sweetman and A. Stannard, Uncertainties in forces extracted from non-contact atomic force microscopy measurements by fitting of long-range background forces., Beilstein J. Nanotechnol. **5**, 386 (2014).
[32] V. Blum, R. Gehrke, F. Hanke, P. Havu, V. Havu, X. Ren, K. Reuter, and M. Scheffler, Ab initio molecular simulations with numeric atom-centered orbitals, Comput. Phys. Commun. **180**, 2175 (2009).
[33] J. P. Perdew, K. Burke, and M. Ernzerhof, Generalized Gradient Approximation Made Simple, Phys. Rev. Lett. **77**, 3865 (1996).
[34] A. Tkatchenko and M. Scheffler, Accurate Molecular Van Der Waals Interactions from Ground-State Electron Density and Free-Atom Reference Data, Phys. Rev. Lett. **102**, 073005 (2009).

[35] L. Jurczyszyn, M. Radny, and P. Smith, Pb chain-like structures on the clean Si(001) surface — A DFT study, Surf. Sci. **605**, 1881 (2011).
[36] H. Yoon, M.-a. Ryu, K.-H. Han, and I.-W. Lyo, Initial growth of Pb on Si at room temperature and low temperature, Surf. Sci. **547**, 210 (2003).
[37] Z.-C. Dong, D. Fujita, and H. Nejoh, Adsorption and tunneling of atomic scale lines of indium and lead on Si(100), Phys. Rev. B **63**, 115402 (2001).
[38] L. Juré, L. Magaud, P. Mallet, and J.-Y. Veuillen, Structure of Pb dimer chains on Si(100)21, Surf. Sci. **482-485**, 1343 (2001).
[39] L. J. Magaud, L. J.-M. G.-R. P. Mallet, and J.-Y. Veuillen, Dynamics of Pb deposits on the Si(100)- 2x1 surface at room temperature, Phys Rev B **61**, 902 (2000).
[40] R. E. Landemark, C. J. Karlsson, Y.-C. Chao, Core-Level Spectroscopy of the Clean Si (001) Surface: Charge Transfer within Asymmetric Dimers of the p(2x1) and c(4x2) Reconstructions, Phys Rev Lett **69**, 1588 (1992).
[41] D. J. Chadi, Atomic and Electronic Structures of Reconstructed Si(100) Surfaces, Phys. Rev. Lett. **43**, 43 (1979).
[42] A. Sweetman, S. Jarvis, R. Danza, J. Bamidele, and E. Al, Manipulating Si(100) at 5K using qPlus frequency modulated atomic force microscopy : The role of defects and dynamics in the mechanical switching of atoms, Phys. Rev. B **84**, 085426 (2011).
[43] Additional information can be found in the online supporting information.
[44] O. E. Dagdeviren and U. D. Schwarz, Accuracy of tip-sample interaction measurements using dynamic atomic force microscopy techniques: Dependence on oscillation amplitude, interaction strength, and tip-sample distance, Rev. Sci. Instrum. **90**, 10.1063/1.5089634 (2019).
[45] J. E. Sader, B. D. Hughes, F. Huber, and F. J. Giessibl, Interatomic force laws that evade dynamic measurement, Nat. Nanotechnol. **13**, 1088 (2018).
[46] K. Morgenstern, N. Lorente, and K.-H. Rieder, Controlled manipulation of single atoms and small molecules using the scanning tunnelling microscope, Phys. Status Solidi B **250**, 1671 (2013).
[47] Y. Sugimoto, A. Yurtsever, N. Hirayama, M. Abe, and S. Morita, Mechanical gate control for atom-by-atom cluster assembly with scanning probe microscopy, Nat. Commun. **5**, 1 (2014).
[48] T.-L. Chan, Y. Ye, C. Wang, and K. Ho, Diffusion of Pb adatom and ad-dimer on Si(100) from ab initio studies, Surf. Sci. **600**, L159 (2006).
[49] M. Krueger, B. Borovsky, and E. Ganz, Diffusion of adsorbed Si dimers on Si(001), Surf. Sci. **385**, 146 (1997).
[50] T.-L. Chan, C. Wang, Z.-Y. Lu, and K. Ho, A first-principles study of Group IV dimer chains on Si(100), Phys. Rev. B **72**, 045405 (2005).